




Accurate Calibration and Measurement of Optoelectronic Devices

Shangjian Zhang , Member, IEEE, Wei Li , Member, IEEE, Wei Chen , Yali Zhang ,
and Ninghua Zhu , Member, IEEE

(Invited Paper)

Abstract—Frequency responses of optoelectronic devices are essential to obtain the precise performance of electrical-to-optical-to-electrical signal conversion or optical signal processing. We reviewed the development of optical or electrical measurement methods proposed for characterizing electrical/optical (E/O) devices, optical/electrical (O/E) devices and optical/optical (O/O) devices in the frequency domain from the perspective of accurate calibration standard. It has been found that full calibrated E/O or O/E measurement requires at least an optoelectronic thru standard for the conversion between optical and electrical domains, and an electrical port extension for de-embedding the error or adapter network of microwave source or detector. The indetermination problem still exists in most O/E and E/O device characterization, which appears in different forms for different measurement techniques. Nevertheless, it should be noticed that obtaining an optoelectronic thru standard can be transferred to characterizing a microwave source or detector in the electrical domain, and a precise electrical calibration standard is much easier to be obtained as compared with an optoelectronic calibration standard. Therefore, the calibration standard transfer from optical to electrical domain is a prominent approach to solve the indetermination problem.

Index Terms—Calibration, electro-optic modulators, frequency response measurement, microwave network analyzer, optical vector network analyzer, photodetectors.

I. INTRODUCTION

OPTOELECTRONIC devices can be categorized as electrical/optical (E/O) devices, optical/electrical (O/E) devices and optical/optical (O/O) devices, including typical directly modulated laser diodes (DMLs), electro-optic intensity

Manuscript received March 28, 2020; revised June 12, 2020; accepted June 24, 2020. Date of publication July 17, 2020; date of current version June 16, 2021. This work was supported in part by the National Key Research and Development Program of China under Grant 2018YFE0201900 and Grant 2018YFB2200700, in part by the National Natural Science Foundation of China under Grant 61927821, Grant 61421002, Grant 61835010, and Grant 60620106013, and in part by the Joint Research Fund of Ministry of Education of China under Grant 6141A02022436. (Corresponding author: Ninghua Zhu.)

Shangjian Zhang and Yali Zhang are with the State Key Laboratory of Electronic Thin Films and Integrated Devices, University of Electronic Science & Technology of China, Chengdu 610054, China (e-mail: sjzhang@uestc.edu.cn; ylzhang@uestc.edu.cn).

Wei Li, Wei Chen, and Ninghua Zhu are with the State Key Laboratory of Integrated Optoelectronics, Institute of Semiconductors, Chinese Academy of Sciences, University of Chinese Academy of Sciences, Beijing 100083, China (e-mail: liwei05@semi.ac.cn; wchen@semi.ac.cn; nhzhu@semi.ac.cn).

Color versions of one or more of the figures in this article are available online at <https://ieeexplore.ieee.org>.

Digital Object Identifier 10.1109/JLT.2020.3010065

modulators (IMs), electro-optic phase modulators (PMs), photodetectors (PDs), optical filters, etc. Optoelectronic devices are essential elements in high-speed optical fiber communications and microwave photonic applications, in which frequency response characteristics of DMLs, modulators and photodetectors are critical to precise electrical-to-optical-to-electrical signal conversion [1], [2], and spectral responses of optical filters are indispensable for hyperfine spectrum manipulation [3].

With the ever-increasing bandwidth requirement of high-speed optical fiber communications and microwave photonic systems, wideband high-resolution optoelectronic device measurement becomes more and more important, since it not only provides effective ways to inspect the device performance, but also bridges the iteration between chip characterization and device packaging. As we know, optoelectronic devices are mainly used for the signal conversion between electrical domain and optical domain. For O/E or E/O devices, frequency responses denote the variation of modulation or demodulation efficiency especially when they are operated at high-frequency regime. For example, the degradation of modulation efficiency at high-frequency modulation is always found in applications of a traveling-wave E/O modulators. The amount of modulation degradation achieved is dependent on the modulation frequency, and related to two key factors: (1) phase-velocity mismatch between light-wave and microwave and (2) impedance mismatch between microwave source and modulator, which are very useful parameters for improving the chip fabrication and device packaging.

In advanced applications such as optical sensing of nanoparticles [4]–[6], optical storage [7], on-chip optical signal processing [8], non-Hermiton parity-time-symmetric quantum mechanics [9], and on-chip optical nonlinear effects [10], the emerging optical components have pushed the requirements for frequency response measurement techniques to an unprecedented level in terms of measurement bandwidth, dynamic range, and especially resolution. For example, an ultra-fine fiber Bragg grating (FBG) with a 3-MHz linewidth [11], optical micro-resonators with ultrahigh quality factor of more than 1000 were successively proposed to improve the sensitivity of the optical sensing system [12] or realize a recording low threshold and narrow linewidth lasing [13]. In this context, the accurate measurement of frequency response of optical devices with ultra-high resolution is a big challenge.

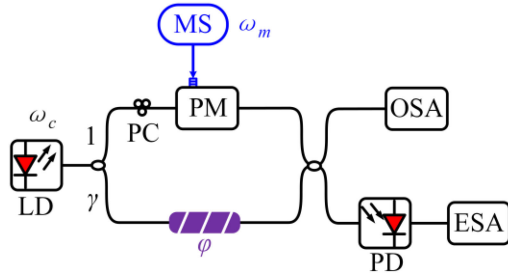


Fig. 1. Schematic diagram for the characterization of an E/O device, LD: laser diode, PC: polarization controller, PM: phase modulator, MS: microwave source, OSA: optical spectrum analyzer, PD: photodetector, ESA: electrical spectrum analyzer.

For the accurate measurement of optoelectronic devices, in this paper, a review about the development of optical or electrical methods for measuring the high-frequency response of optoelectronic devices is presented. Sections II and III provide summative introductions to the typical measurement techniques for E/O modulators and O/E photodetectors. Section IV introduces the frequency response measurement of O/O devices. In Section V, we investigate for the first time to our knowledge the optoelectronic measurement methods from the perspective of transfer of calibration standard, which provides more informative angle of view to the calibrated frequency response in both optical and electrical domain. Future lines of optoelectronic measurement are discussed and outlooked together with main conclusion provided in Section VI.

II. E/O DEVICE MEASUREMENT

There are two main methods to load an electrical signal onto an optical carrier, namely external modulation and direct modulation. External modulation transfers the electrical signal to optical domain with the use of a separate modulator, such as a Mach-Zehnder modulator (MZM), an electro-absorption modulator (EAM) and an electro-optic PM, wherein the Lithium Niobate (LiNbO₃)-based MZMs and PMs are widely used E/O devices with the advantages of linear electro-optic effect, larger bandwidth and reduced chirp. In a DML, the electrical signal is placed on the optical carrier by modulating laser current, which brings relatively low-cost level and reduced system complexity.

The frequency responses of E/O devices are typically measured with optical spectrum analysis method, electrical spectrum frequency-swept method, and optical heterodyne frequency-converted method. As shown in Fig. 1, an optical carrier at the angular frequency ω_c in the upper branch of an interferometer is modulated in the PM at the microwave frequency ω_m . The same carrier in the lower branch is phase shifted by φ , and the combined optical signal at the output of the interferometer can be written by

$$\begin{aligned} E(t) &= E_c e^{j\omega_c t} \cdot \left(e^{jm(\omega_m) \sin \omega_m t} + \gamma e^{j\varphi} e^{j\psi} \right) \\ &= E_c e^{j\omega_c t} \cdot \left\{ \sum_{n=-\infty}^{+\infty} J_n [m(\omega_m)] e^{jn\omega_m t} + \gamma e^{j(\varphi+\psi)} \right\} \end{aligned} \quad (1)$$

with the amplitude E_c of the optical carrier, the modulation depth m of PM at the modulation frequency ω_m , and the relative amplitude γ and phase ψ between the two interferometer branches, respectively. Then the combined optical signal is sent to an optical spectrum analyzer (OSA) and a PD, respectively. The generated photocurrent after photodetection can be expressed as

$$\begin{aligned} i(t) &= R \cdot |E(t)|^2 = R \cdot \left\{ (1 + \gamma^2) E_c^2 + 2\gamma E_c^2 \right. \\ &\quad \left. \cdot \sum_{n=-\infty}^{+\infty} J_n [m(\omega_m)] \cos(n\omega_m t - \varphi - \psi) \right\} \end{aligned} \quad (2)$$

with the responsivity R of the PD. In the case of $\gamma = 0$, the interferometer only consists of a PM, and the photocurrent only includes DC component from Eq. (2). Therefore, PMs are often measured with an OSA by analyzing the relationships between the optical carrier and its sidebands based on Eq. (1). In the case of $\gamma \neq 0$ and $\varphi = \text{constant}$, the interferometer represents a basic MZM, and the frequency component at ω_m after photodetection can be easily quantified as

$$\begin{aligned} i(\omega_m) &= 4\gamma E_c^2 R(\omega_m) J_1 [m(\omega_m)] \sin(\varphi + \psi) \\ &\propto R(\omega_m) J_1 [m(\omega_m)] \end{aligned} \quad (3)$$

From Eq. (3), a MZM can be characterized in the electrical domain with the help of a reference PD. In other words, the electrical spectrum frequency-swept method can be used to measure the cascaded response of MZMs and PDs, and the accuracy relies on the calibration to de-embed the impact of the reference PD for characterizing an E/O device or to de-embed the impact of the reference MZM for characterizing an O/E device.

The optical spectrum analysis method was firstly proposed by F. Auracher and R. Keil [14]. Later, T. Kawanishi and S. Oikawa demonstrated half-wave voltage ($V\pi$) measurements of MZMs under small-signal approximation model based on the optical spectrum analysis [15], [16]. In 2003, Y. Q. Shi *et al.* improved the theory of optical spectrum analysis, and made it a fundamental method for extracting half-wave voltages of PMs and MZMs [17]. The measurement setup includes only an optical source, a microwave source and an optical spectrum analyzer together with the modulator under test. As shown in Fig. 2(a), the optical spectrum analysis is focused on the relationships between the optical carrier and its sidebands, corresponding to the case of $\gamma = 0$ in Fig. 1. The approaches exploit the high sensitivity and large dynamic range of an optical spectrum analyzer (OSA) and allows E/O device characterization from low (small signal) to high (large signal) driving power levels. In 2004, N. Courjal *et al.* demonstrated the extinction-ratio-independent method for chirp measurements of MZMs based on the optical spectrum analysis [18]. In 2005, L. S. Yan *et al.* proposed the graphical solution for half-wave voltage and chirp parameters of MZMs using optical spectrum analysis [19]. In 2006, we extended the optical spectrum analysis method to extracting frequency responses of DMLs [20], [21], as shown in Fig. 2(b).

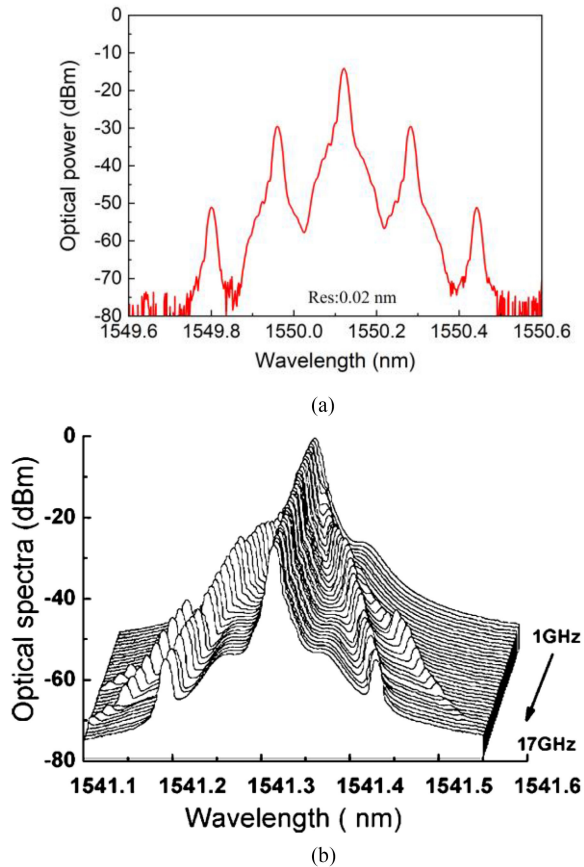


Fig. 2. Typical optical spectrum of (a) an externally modulated optical signal and (b) a directly modulated optical signal [21].

In 2009, Y. Liao *et al.* realized the frequency response measurement at high frequency for MZMs through the power ratio between high-order modulation sidebands in the optical spectrum [22]. In 2014, C. Yang *et al.* used similar method to measure half-wave voltages of PMs [23]. Up to now, the optical spectrum analysis is still considered as a very simple and effective method, enabling the direct measurement of absolute frequency responses for DMLs, MZMs and PMs in the optical domain. Nevertheless, the spectrum measurement in the optical domain is often affected by the linewidth of the laser source and the resolution of the commercial OSA, which is limited to be with low resolution of about 0.02 nm at around 1550 nm.

For high-resolution measurement, R. F. Bauer and JR. P. Penfield introduced the electrical spectrum frequency-swept method into optoelectronic measurement, and developed the de-embedding technology for measuring frequency response of optoelectronic devices based on the widely-used microwave network analyzer [24]. In 2003, P. D. Hale and D. F. Williams described the procedure for characterizing a large class of O/E or E/O devices with a calibrated microwave network analyzer and a calibrated reference O/E transducer [25], since the electrical measurement relies on intense calibration to de-embed the impact of the reference PD in the measured frequency response, or expensive equipment, such as a light-wave component analyzer (LCA) with built-in calibrated reference O/E

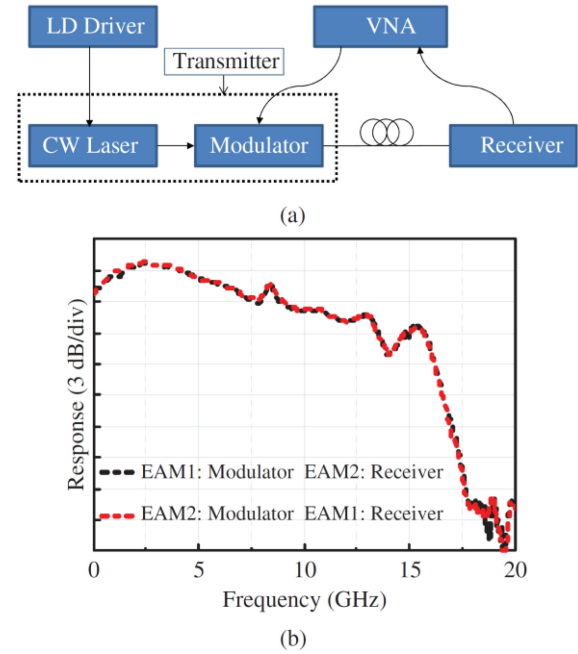


Fig. 3. (a) Experimental setup for proving the quasi reciprocal approximation of frequency response of EAM as a modulator or a photodetector. CW: continuous wave. LD: laser diode. (b) Results of experiments in Fig. 3(a) [27].

transducers, corresponding to the case of $\gamma \neq 0$ and $\varphi = \text{constant}$ in Fig. 1. In 2009, we proposed microwave generation in an electro-absorption modulator with a DFB laser subject to optical injection [26]. From the experiment, it has been found that when the EAM modulator is used as a photodetector or a modulator, its frequency responses are almost identical. In order to simplify the E/O calibration, we proposed quasi reciprocal approximation based on the fact that an EAM can be used for E/O modulation and O/E photodetection with the same frequency response, as shown in Fig. 3(a) and (b), and demonstrated measuring the frequency responses of a DML and a MZM with the help of an EAM as the assisted modulator and photodetector [27], [28]. The experiments show the frequency responses measured by this method only contain the characteristics of the devices under test without the influence of other assistant devices.

With similar scheme, a phase modulator can also be frequency-swept measured in the electrical spectrum after the phase modulation-to-intensity modulation (PM-to-IM) conversion. Several kinds of optical structure have been used to realize PM-to-IM conversion, such as a polarization interferometer [29], a Sagnac loop [30], the dispersion in fibers [31], a Mach-Zehnder delayed interferometer, and a tunable optical bandpass filter [32], [33]. However, most of these PM-to-IM conversion methods assume that the photodetection has an ideal flat frequency response in the measurement system in the concerned frequency range, which should be corrected through an extra O/E calibration for the photodetection.

Recently, with the development of tunable lasers, optical heterodyne methods have been widely investigated, which was also proposed by F. Auracher for measuring the high frequency modulation characteristics of MZMs [14]. The optical heterodyne

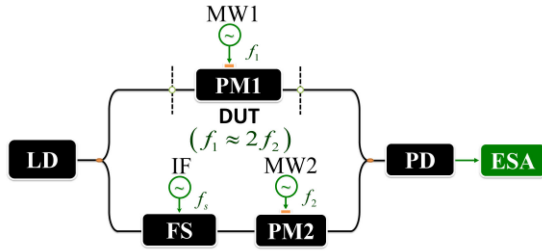


Fig. 4. Schematic diagram of the proposed frequency-shifted heterodyne method. LD, laser diode, PC, polarization controller, PM1, phase modulator under test, PM2, secondary phase modulator, FS, frequency shifter, MW, microwave source, DUT, device under test, PD, photodiode, ESA, electrical spectrum analyzer, OSA, optical spectrum analyzer [38].

method was also used by T. S. Tan to simultaneously measuring both the modulator and the photodetector [34]. In 2006, A. K. M. Lam developed optical heterodyne frequency-converted method and realized the high frequency response of MZMs [35]. In 2007, A. A. Chtcherbakov improved the optical heterodyne frequency down-converted method and achieved both the amplitude and phase frequency response of MZMs [36]. In 2010, C. E. Rogers III employed the optical heterodyne method to characterize the residual chirp of a MZM [37].

For high-resolution measurement of PMs, we proposed a self-calibrated heterodyne scheme. From Eq. (2), in the case of $\gamma \neq 0$ and $\varphi = \varphi(t) = \omega_s t$, the frequency components can be obtained as following

$$i(\omega_m - \omega_s) = 2\gamma E_c^2 R(\omega_m - \omega_s) J_1[m(\omega_m)] \quad (4a)$$

$$i(\omega_s) = 2\gamma E_c^2 R(\omega_s) J_0[m(\omega_m)] \quad (4b)$$

For a self-calibrated E/O measurement, the sweeping microwave signal ω_m on the PM is set close to twice of the frequency ω_s ($\omega_m \approx 2\omega_s$), so that the assumption on the responsivity $R(\omega_m - \omega_s) \approx R(\omega_s)$ is satisfied. Thus, the modulation index of PM can be extracted from

$$H[m(\omega_m)] = \frac{i(\omega_m - \omega_s)}{i(\omega_s)} = \frac{J_1[m(\omega_m)]}{J_0[m(\omega_m)]} \quad (5)$$

In practice, the frequency-shifted optical heterodyne method was demonstrated as shown in Fig. 4 [38], consisting of an acousto-optic frequency shifter and two PMs located in a Mach-Zehnder interferometer (MZI). The two PMs are separately driven by different microwave signals with about half frequency relationship. The modulation efficiency of PM under test is extracted from the beat note of the detuned optical carriers and the modulated sidebands. The uneven responses of the PD are cancelled out through keeping the half frequency relationship of the driving microwave signals, and thus a self-calibrated E/O measurement can be achieved, as shown in Fig. 5(a) and (b). In 2017, we demonstrated a four-in-one measurement based on the frequency-shifted heterodyne scheme for frequency response measurements of high-speed optoelectronic devices with a shared self-heterodyne interferometer [39], given in Fig. 6, including the modulation index of LDs, modulation index, half-wave voltage and chirp parameter of MZMs, modulation index

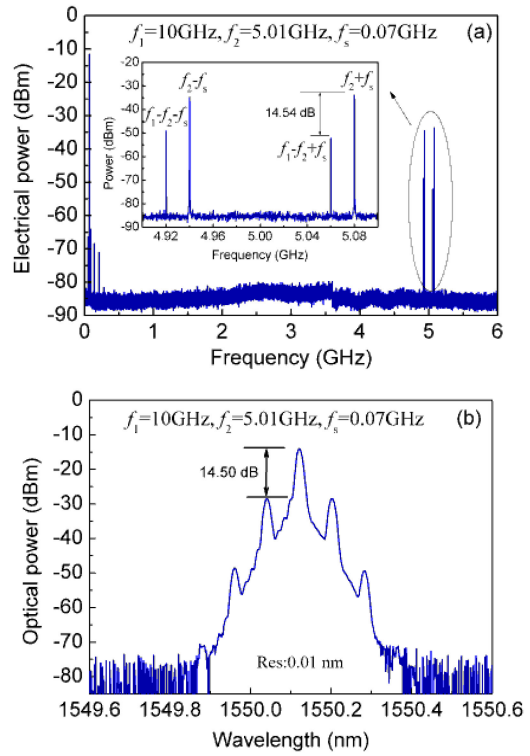


Fig. 5. (a) Measured electrical spectrum of the heterodyning signal and (b) the corresponding optical spectrum of PM1 [38].

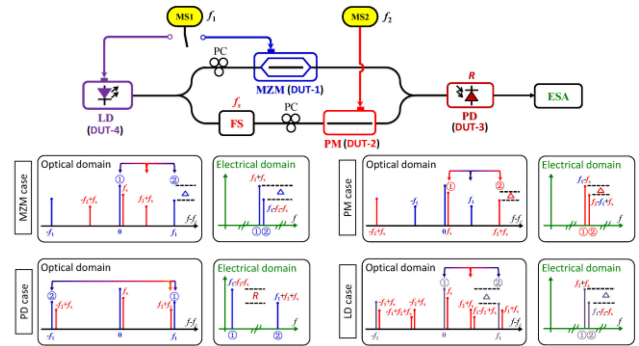


Fig. 6. Schematic setup of the self-calibrated frequency response measurement method. LD, Laser diode, FS, Frequency shifter, MZM, Mach-Zehnder modulator, PM, Phase modulator, PD, Photodetector, PC, Polarization controller, ESA, Electrical spectrum analyzer, MS, Microwave source. The insets show the equivalent spectrum mapping from optical domain to electrical domain for every device under test [39].

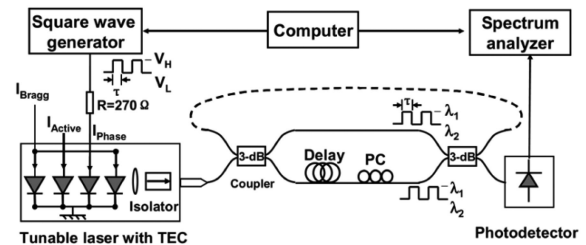


Fig. 7. Improved self-heterodyne method for measuring the frequency response of PDs, PC: polarization controller [44].

and half-wave voltage of PMs, and responsivity of PDs, which is free of any extra E/O calibration for the assisted devices except the device under test. In order to characterize on-chip devices, we presented electrical probing testing based on serial or parallel modulation mixing for characterizing high-speed transceiving devices with self-reference and on-chip capability [40]. The testing can also avoid the extra O/E or E/O correction, and allow electrical probing with reduced or free of optical coupling off chip, enabling this serial or parallel modulation mixing method promising for on-chip measurement of wafer level devices or circuits.

III. O/E DEVICE MEASUREMENT

Frequency response measurement of O/E devices can be categorized into all-optical stimulus method and electro-optic stimulus method. All-optical methods typically include the optical heterodyne method and the intensity noise method [41]–[43]. The principle of the optical heterodyne method is based on the beat frequency, with which J. Wang constructed a delayed self-heterodyne structure of DML and achieved the high-frequency measurement for the responsivity of PD [42]. In 2006, we proposed a delayed self-heterodyne method based on a distributed Bragg-reflector (DBR) semiconductor laser to obtain the high-frequency responsivity of PD [44]. The linewidths at the frequencies corresponding to the beat peaks have been used to correct the measured frequency response, and the measurement accuracy can therefore be significantly improved. The optical method with the self-reference capability is the intensity noise method based on an amplified spontaneous emission (ASE) source, in which the ultrawide optical spectrum from ASE is directly put into the high-speed PD under test and the beating among them allows to extract the frequency response of PD in the ultra-wide frequency range. This method works without any microwave component but suffers from the poor signal-to-noise ratio.

Different from all-optical stimulus method, the principle of electro-optical stimulus method is based on the electro-optical source originated from the electro-optic modulation. In 2005, M. Yoshioka proposed a secondary intensity modulation method for the high-frequency measurement of the high-speed PD [45]. However, this method was seriously influenced by the bias drifting of the modulators. In 2012, K. Inagaki developed one dual-frequency laser source formed by the carrier-suppressed double sideband modulation to realize the high-frequency measurement for the PD [46]. Prior to the all-optical method, the electro-optic method can quickly and simply obtain the frequency response of the high-speed PD by using a microwave network analyzer through the cascaded E/O device and O/E device network [47]. Nowadays, the electrical spectrum frequency-swept method has been widely used in measuring PDs [48]. Nevertheless, it should be noted that the measured results from the microwave network analyzer is the frequency response of the whole cascaded network, as given by Eq. (3). Extra E/O calibration is always required to subtract the frequency response of the assistant modulator to extract the responsivity of the PD itself. To address this dilemma, we extended the electrical spectrum frequency-swept method based on quasi reciprocal approximation [27]. As mentioned in Section II, we made the best of an EAM which

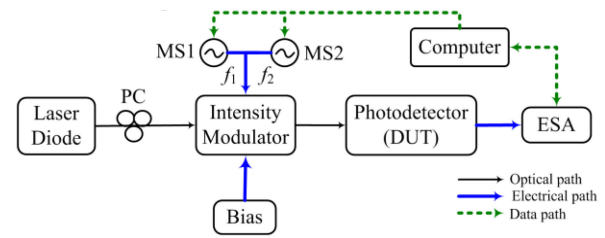


Fig. 8. Schematic of the two-tone mixing for measuring PDs. MS: microwave source, DUT: device under test, PC: polarization controller, ESA: electrical spectrum analyzer [50].

can be used as a modulator and photodetector with the same frequency response, and demonstrated measuring the frequency responses of an EAM and a PD with the help of the EAM as a modulator and a photodetector [28].

In 2015, we extended the frequency-shifted heterodyne scheme to measure frequency response of PDs [49]. The electro-optic stimulus consists of an acousto-optic frequency shifting and two-tone phase modulation in a MZI structure. The two-tone phase modulation generates multiple pairs of sum-and-difference sidebands with equalized amplitude in the optical domain, regardless of driving levels of the PMs. The frequency-detuned optical carrier heterodynes with two pairs of sidebands in the electrical domain after photodetection, from which the frequency response of PD is extracted without any extra E/O calibration. Note that the method is applicable for different driving levels and operating wavelengths, since it is established without any small-signal assumption. In 2016, we simplified the electro-optic stimulus based on two-tone intensity modulation [50]. As is shown in Fig. 8, the method consists of a MZM driven by two closely spaced sinusoidal tones. The two-tone intensity modulation generates the harmonic sidebands in the optical spectrum and their sum-and-difference frequency products in the electrical spectrum after photodetection allows direct extraction of frequency responses of PDs.

In 2019, S. L. Pan *et al.* proposed the frequency response measurement for integrated coherent receivers based on the optical carrier-suppressed double-sideband (ODSB) modulation and optical carrier frequency shifting. The measured results were calibrated through the optical power measurement for the desired optical carrier and sidebands [51].

Recently, we proposed an ultra-wideband and frequency scalable electro-optic stimulus for self-referenced measurement of high-speed PDs through segmental up-conversion based on low-speed photonic sampling [52], with the help of a low-repetition-frequency mode-locked laser diode (MLLD), as shown in Fig. 9. It achieved ultra-wide and scalable frequency response measurement of PDs with $2M$ -fold measuring frequency range, where the sweeping frequency up to $N \times f_r/2$ of the modulator enables the measuring frequency range of $M \times N \times f_r$ ($M = 10$, $N = 51$).

IV. O/O DEVICE MEASUREMENT

In recent decades, a series of techniques have been proposed to realize the simultaneous measurement of magnitude and phase responses of optical device under test (ODUT), as are called optical vector analysis (OVA). Conventional OVAs were basically

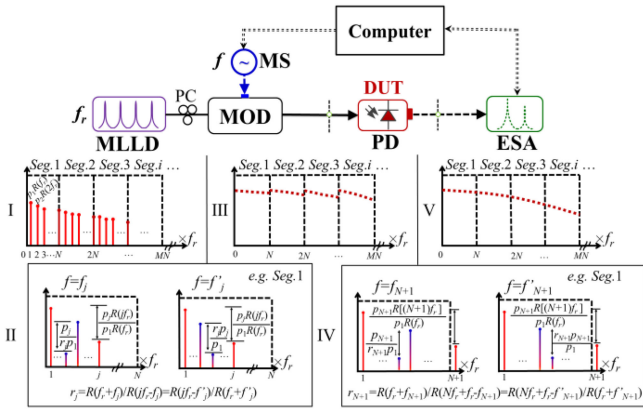


Fig. 9. Schematic diagram of the low-speed photonic sampling, MLLD: mode-locked laser diode, MOD: modulator, MS: microwave source, DUT: device under test, PD: photodetector, ESA: electrical spectrum analyzer [52].

implemented based on optical methods including the modulation phase-shift method [53] and the interferometric method [54], [55] using a wavelength-swept laser source. These methods are advantageous for the ultra-wide measurement frequency range and the large dynamic range. However, due to the limited wavelength accuracy of state-of-the-art laser sources, a typical resolution of only 1.6 pm (around 200 MHz in 1550-nm waveband [55]) can be achieved, making it powerless for the measurement of ultrafine ODUTs. In order to obtain high-resolution optical spectrum responses, researchers have also turned to develop approaches that obtain the optical spectrum responses of ODUTs in the electrical domain via the optical-to-electrical and electrical-to-optical conversion. One kind of such OVAs are realized based on a digital signal processing (DSP), whose basic idea is just similar to the methods used for the optical channel estimation [56]–[62]. By transmitting coherent optical orthogonal frequency division multiplexed (OFDM) symbols through an ODUT and then comparing the received symbols with the original ones, the response of ODUT can be calculated. In these DSP-based OVAs, the use of the narrow linewidth laser source and the fast Fourier transformation on a large number of points have ensure a fast and high-resolution measurement (e.g., a resolution of 5.86 MHz in 1.45 microseconds [60]). However, due to the limited signal to noise ratio (SNR) of OFDM signals, the obtained dynamic range in a one-time measurement is relatively small and it can be further smaller as the resolution increase. For example, the achieved dynamic range is 15 dB at a resolution of 5.86-MHz in [62], which is too small to measure the high-Q optical components. In addition, the limited SNR of OFDM signals also make it nearly necessary to repeat the measurement for tens of times to reduce the measurement error, which in turn lower the measurement speed.

Subsequently, OVAs based on the optical single sideband (SSB) modulation have been proposed and developed to achieve both a high resolution and large dynamic range [63]–[79]. Optical SSB modulated signal can carry the information of optical spectrum responses of an ODUT after passing through it. The beating between the optical carrier and its first-order sideband in the PD can thus establish a point-to-point mapping between

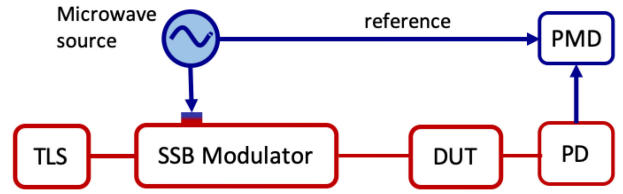


Fig. 10. Schematic diagram of a typical OVA based on optical single sideband (SSB) modulation. TLS: tunable laser source, DUT: device under test, PD: photodetector, PMD: phase and magnitude detector.

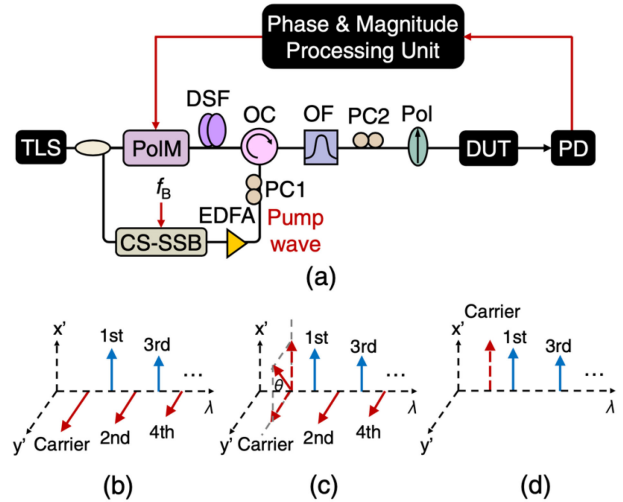


Fig. 11. Illustration of accuracy-improved SSB-OVA based on suppression of even-order sidebands. (a) the system setup, PolM: polarization modulator; CS-SSB: carrier suppressed single sideband; DSF: dispersion shifted fiber; OC: optical coupler; OF: optical filter; PC: polarization controller; Pol: polarizer; EDFA: erbium doped fiber amplifier. (b)–(d) schematic diagram of the optical signal spectrum [71].

the optical and electrical domain. As a result, the responses of ODUT can be obtained by detecting the magnitude and phase of the photocurrent from the PD. Fig. 10 shows the schematic diagram of a typical OVA based on SSB modulation. Thanks to the stable and accurate radio frequency (RF) technology, the resolution of SSB-OVAs can reach sub-kHz. Generally, SSB modulation can be realized with the assistance of a 90° hybrid coupler [63]–[67], an optical bandpass filter [68], or nonlinear effects such as the stimulated Brillouin scattering (SBS) [69]. In these schemes, the undesired sidebands cannot be eliminated perfectly, whose beating with the optical carrier will introduce considerable measurement errors. In addition, to achieve larger dynamic range, the modulation index should be large enough to ensure a large enough power of the desired optical sideband, which will also lead to a series of high-order sidebands. As a result, the beating between high-order sidebands will significantly constitute another source of the measurement errors. To improve the measurement accuracy of SSB-OVAs, M. Xue [70], [71] and W. Wang [72] have proposed methods based on the direct error subtraction, and we have proposed methods based on the suppression of even-order sidebands [73], [74]. Fig. 11(a) shows the system setup of an accuracy-improved SSB-OVA using Brillouin-assisted polarization pulling, and Figs. 11(b)–(d)

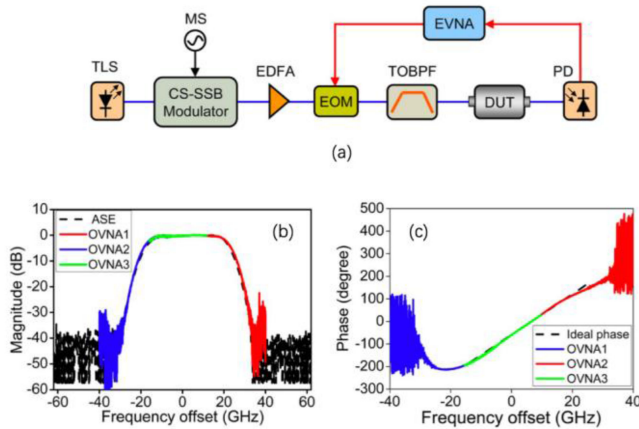


Fig. 12. SSB-OVA with extended measurement range based on segmental measurement. (a) the system setup, EOM: electro-optical modulator; MS: microwave source; EVNA: electrical vector network analyzer. The measured (b) magnitude and (c) phase response of DUT [74].

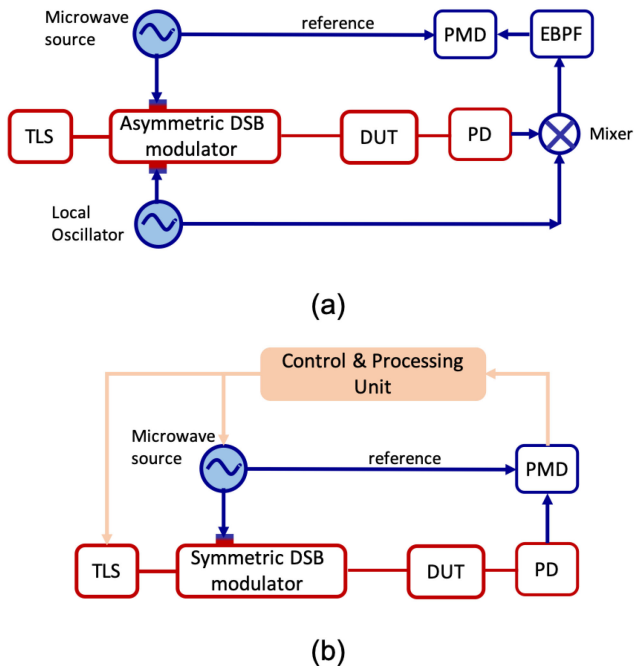


Fig. 13. Schematic diagrams of OVAs based on (a) carrier-frequency-shifted double sideband (DSB) modulation and (b) symmetric DSB modulation. TLS: tunable laser source; DUT: device under test; PD: photodetector; PMD: phase and magnitude detector; EBPF: electrical band-pass filter.

show the schematic diagram of optical signal spectrum during the generation of SSB signal with suppression of even-order sidebands. These methods have made a big progress to avoid the tradeoff between large dynamic range and low measurement error. SSB-OVAs with extended measurement range have also been proposed based on SSB modulation using the second-order sideband [75] or an optical frequency comb (OFC) [76]. In 2014, we proposed a method based on the segmental measurement to characterize ODUTs with a bandpass response [77], the system setup of which is shown in Fig. 12(a). Figs. 12(b) and 12(c) show the measured magnitude and phase response, respectively.

Despite so much effort, the measurement range of SSB-OVAs with a single optical carrier cannot exceed the device bandwidth while maintaining a high resolution. Moreover, the measurement of bandpass ODUT in a relatively simple manner remains a great challenge.

In this context, OVA based on the double sideband modulation (DSB) have been proposed to overcome the disadvantages of SSB-OVAs. Generally, optical DSB modulated signal cannot be used to perform the point-to-point mapping between the optical and electrical domain, since the beating between the optical carrier and the two first-order sidebands will alias in the PD at the same frequency. In 2013, M. Wang and J. Yao demonstrated an OVA based on the unbalanced DSB modulation with an asymmetric power of the two first-order sidebands [78]. Similarly, T. Qing *et al.* have proposed a scheme based on the carrier-frequency-shifted DSB modulation [79]–[81]. The DSB modulation involved in the above schemes are specially designed to be asymmetric in terms of frequency or power. The problem of beating aliasing which normal DSB modulated signals suffer from can thus be solved, however, at the cost of much more system complexity caused by the asymmetric DSB modulated signal generation or the frequency-shifted signal detection. Asymmetric DSB-OVA has also been proposed based on the electro-optical harmonics heterodyne [82]. Owing to the use of Wiener-Lee transformation, only magnitude detection is required in the system, which greatly reduced the complexity of the detection. In 2017, we proposed for the first time an OVA based on the symmetric DSB modulation using a dual-parallel Mach-Zehnder modulator (DPMZM) [83]. By measuring the ODUT multiple times under different optical carrier phase shift (CPS) and post-processing the measurement results, the responses of the ODUT can be obtained accurately.

Similar symmetric DSB-OVAs were also demonstrated using a polarization modulator (PoLM) [81], a dual-drive MZM [85], or a pair of intensity modulator and a phase modulator [86]. Figs. 12(a) and 12(b) show the schematic diagrams of the DSB-OVAs based on the carrier-frequency-shifted method and the CPS method, respectively. It can be seen that the CPS-based scheme dramatically simplified the system of DSB-OVAs since no extra modulator, electrical filter, RF mixer, or RF source are required in symmetric DSB modulation. In 2019, we have further proposed an accuracy-enhanced scheme to overcome the uncertainty of CPS in DSB-OVAs [87]. Compared with SSB-OVAs, these DSB-OVAs have doubled the measurement range with a single optical carrier while maintaining the high resolution. On this basis, DSB-OVAs have also opened up a new chapter of an OVA being suitable for the measurement of the arbitrary response.

Generally, if the ODUT has a birefringence feature, we can also apply the aforementioned methods in two orthogonal polarization states by adding polarization control, and then calculate the polarization-dependent parameters according to the Jones matrix [88]–[90]. There should also be an important reminder that the aforementioned methods are not contradictory to each other, and they can be combined to exert greater advantages. For example, a few months ago in 2019, T. Qing and S. Pan have demonstrated an OVA with attometer resolution, 90-dB dynamic

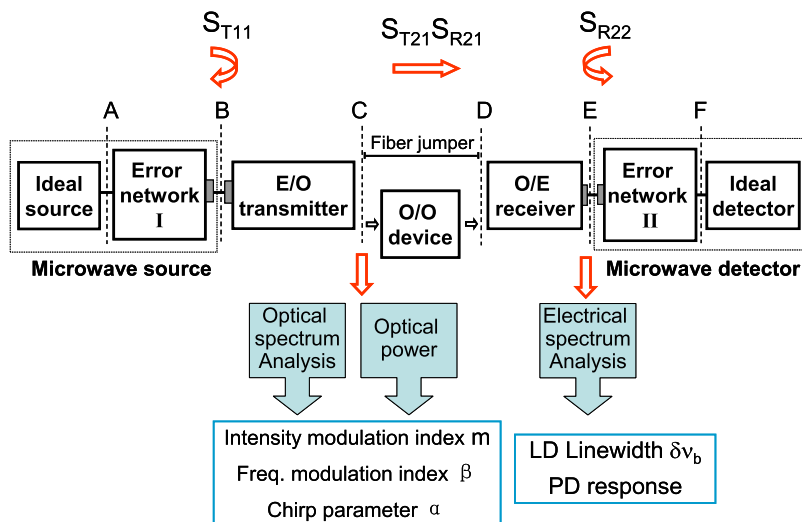


Fig. 14. Errors in the frequency response measurement of optoelectronic devices.

range and THz bandwidth by combining the advantages of the asymmetric DSB-OVA and the OFC-based OVA [91].

V. TRANSFER OF CALIBRATION STANDARD

From the summative introduction, the electrical spectrum frequency-swept methods have been proved to be powerful for measuring both modulators and photodetectors, with the help of a high-resolution microwave network analyzer. However, we always encounter a cascaded network of E/O and O/E devices. To accurately measure the response of an E/O device, a known reference O/E device as a calibration standard must be used, and vice versa. Therefore, obtaining an accurate either E/O or O/E calibration standard is the problem we must overcome.

In order to obtain the first calibration standard, many methods have been proposed in the characterization of individual E/O or O/E device. The procedures are quite similar to the calibration of non-reciprocal test fixtures in the electrical domain [92]. It will be very attractive if a similar approach can be applied to the optoelectronic device measurement. Unfortunately, the general circuit theory shows that no matter how many and what type of calibration standards are used, the individual transmission coefficients cannot be determined. Let us call this indetermination problem. However, the understanding of this issue is not explicit, and many efforts have been attempted to solve this problem. For example, a bilateral electro-optic network (BEON) which allows forward (E/O) and reverse (O/E) transmissions has been constructed [93]–[95]. In fact, the indetermination issue is still unsolved because the constructed bidirectional network is non-reciprocal.

Fig. 14 shows the possible error sources in the measurement of optoelectronic devices. The error sources are divided into four parts. Error boxes I and II indicate the errors of microwave source and detector, and the errors from E/O and O/E devices are included in the optical transmitter and receiver, respectively. The O/O devices can be a long optical fiber, or an optical modulated laser, etc. In the calibration of the measurement setup,

the O/O device can be replaced by a short fiber jumper, which has a flat frequency response. In the following, we summarize the various methods for characterizing the individual E/O or O/E device.

Microwave network analyzer has become a key instrument for the S-parameter measurement of microwave networks [26]. A set of calibration standards, such as short, open, matched load, thru, and delay line, can be used to remove completely the errors of test fixtures, the microwave source and the detector, and locate the test reference planes at “B” and “E” [96]. For an optoelectronic network cascaded by E/O and O/E devices, the parameters which can be measured are S_{T11} , $S_{T21}S_{R21}$ and S_{R22} , and individual parameter S_{T21} or S_{R21} can not be determined. For a reciprocal network, the extended short-open-load method can be used to uniquely determine the individual transmission coefficients S_{21} and S_{12} [97]. Unfortunately, the constructed bidirectional network BEON is non-reciprocal. Therefore, the indetermination problem can not be solved with a similar calibration technique using three reflection standards. Lightwave component analyzer (LCA) is developed based on the microwave network analyzer. In principle, the indetermination issue still exists. LCA can be used to measure optical/optical (O/O) device after the O/O calibration. In this case the test reference planes are at “C” and “D”.

Small-signal power measurement is based on the nonlinearity of a MZM or an EAM [98]–[100]. The high-frequency modulation index can be extracted from the measured optical output power. In the measurement, the high-speed PD and the broadband microwave detector are not required. However, the response of the driving microwave source is still involved in the measured results, and the test reference planes can only be located at “A” and “C”.

In the optical heterodyne method for characterizing the high-speed PD, the effects of the electrical spectrum analyzer can not be removed, and the test reference planes are at “D” and “F”. Optical heterodyne technique can also be used to measure the frequency response of the optical modulator, and the test

reference planes can be located at “A” and “F”. Through E/E calibration, the reference test planes can be moved further to “B” and “E”.

In the impulse response technique [101], the test reference planes can only be moved to “A” and “F”, because the response of the oscilloscope can not be subtracted from the measured results.

The optical spectrum analysis technique is very attractive because the measurement frequency range depends only on the microwave source and there is no need to use a calibrated broadband PD. However, the response of the microwave source is still affecting the measured results.

With the frequency-shifted heterodyne scheme, the E/O measurement can be achieved without the requirement of extra O/E calibration, which corresponds to the reference plane moved to “A” and “C”. Similarly, the O/E measurement can be operated at the reference plane between “D” and “F”. Note that the error network I from microwave source and the error network II from microwave detector are still needed to de-embedding for the completed calibrated results of the intrinsic E/O or O/E device.

VI. DISCUSSION AND CONCLUSION

Network analyzer calibration is one of the most important steps in microwave network measurement. Accuracy depends on the precision of calibration standards and methods. Short, open, match, thru (or delay) are always used as calibration standards. A lot of methods, such as the line-short-open (LSO), thru-reflect-line (TRL), thru-short-match (TSM), thru-open-match (TOM) etc., have been developed for a two-port calibration. All these methods need at least one transmission standard, such as standard thru or line. It is easy to achieve these standards if the test ports of the devices are identically electrical or optical. For example, in the O/O device measurement, the standard thru or line can be easily obtained by simply removing the ODUT and connecting the two optical ports of the OVA directly. Therefore, the conventional optical measurement for O/O devices can be smoothly shifted to the electrical domain, with only neglectable effect from the microwave source and microwave detector. The frequency response calibration in the O/O device measurement is focused on the reduction of measurement errors induced by the nonlinearity of the modulator, in order to keep establishing a linear point-to-point spectrum mapping between the optical and electrical domain. In addition, more efforts have also been paid to the dynamic range improvement and the measurement range increase.

In the case of the E/O or O/E device measurement, the thru calibration standard is far from obtainable, because the two test ports are one electrical port and one optical port, belonging to different domains. Therefore, the measured frequency response often includes not only the individual contribution from the E/O and O/E devices under test, but also the inevitable influence from the driving microwave source and the detecting microwave receivers. For example, the full calibration in the E/O measurement requires at least two necessary procedures. The first one is to realize the self-reference O/E conversion from optical domain to electrical domain, corresponding to the test plane shifting

from “F” to “C”, and the second one is to obtain electrical calibration at the electrical port of E/O device, corresponding to the test plane shifting from “A” to “B”. Thus, the reference plane can be located at “B” and “C”, from which we can obtain the frequency response of the E/O modulator itself. Similar analysis can be applied to the O/E device case, corresponding to the test reference plane to “D” and “E”, respectively.

From the analysis in Section V, there is still work to move the reference planes to “B” and “C” for the E/O device measurement, or to “D” and “E” for the O/E device measurement, the indetermination problem still exists in the aforementioned methods, but appears in different forms. Nevertheless, it should be noticed that with the developed methods, obtaining an E/O or O/E standard can be transferred to characterizing a microwave source or a detector in the electrical domain. It is well known that a precise electrical calibration standard is much easier to be obtained as compared with an optoelectronic calibration standard. Therefore, the calibration standard transfer from optical domain to electrical domain is a prominent approach to solve the indetermination problem.

The quasi reciprocal approximation, we think, provides useful ideas to solve the indetermination problem, in terms of transferring the calibration standard. As we know, for symmetric reciprocal networks, the frequency response characteristics can be obtained by measuring the S-parameters of cascaded symmetric reciprocal networks. It has been observed that a reversely biased EAM can be used as a dual-functional device for modulation and detection in the optoelectronic transceiver applications. Moreover, lots of experiments have been demonstrated that when the EAM is used as a PD or a MOD, its frequency responses are almost identical [26]–[28]. Therefore, the EAM can be considered as a candidate of reciprocal network. It is worth noticing that the EAM must be terminated with good impedance matching for better accuracy, since the driving microwave source and receiving detector are already matched with $50\ \Omega$ at the input or output port.

At present, optoelectronic devices are playing increasingly important roles in photonics-assisted microwave measurement and instrumentation [102], in contrast, the high-frequency measurement of optoelectronic devices is still continuing the lines of thinking of electronic devices. With the continuous progress of electrical instrumentation, we may find new mechanisms and practical solutions. For example, the NIST electrooptic sampling system has been proposed to measure the complex band-limited Fourier transform of the electrical impulse response of a fast PD to 110 GHz [103], [104]. These PDs, when stimulated with a short optical pulse, are then capable of delivering well-characterized pulses to their electrical loads and can be used to provide traceable calibrations for LCAs, sampling oscilloscopes, large-signal network analyzers. There are also some measurement uncertainties in the electrooptic sampling system, which are caused by the response time of LiTaO₃ wafer, the pulse width and waist size of the light, the transmission depth of electric field and the multiple reflection of the light. However, the electrooptic sampling scheme provides a method to accurately measure high-speed PDs, which may provide a scientific way to solve the indetermination problem in the optoelectronic device measurement.

REFERENCES

- [1] N. H. Zhu *et al.*, "Directly modulated semiconductor lasers," *IEEE J. Sel. Topics Quantum Electron.*, vol. 24, no. 1, pp. 1–19, Jan.-Feb. 2018.
- [2] J. Capmany and D. Novak, "Microwave photonics combines two worlds," *Nature Photon.*, vol. 1, no. 6, pp. 319–330, Jun. 2007.
- [3] J. Yao, "Microwave photonics," *J. Lightw. Technol.*, vol. 27, no. 3, pp. 314–335, Feb. 2009.
- [4] Y. Zhi, C. Xiao, Q. Gong, L. Yang, and Y. Xiao, "Single nanoparticle detection using optical microcavities," *Adv. Mater.*, vol. 29, no. 12, Mar. 2007, Art. no. 1604920.
- [5] F. Vollmer, and S. Arnold, "Whispering-gallery-mode biosensing: label-free detection down to single molecules," *Nature Methods*, vol. 5, no. 7, pp. 591–596, Jul. 2008.
- [6] M. D. Baaske, M. R. Foreman, and F. Vollmer, "Single-molecule nucleic acid interactions monitored on a label-free microcavity biosensor platform," *Nature Nanotechnology*, vol. 9, no. 11, pp. 933–939, Nov. 2014.
- [7] L. Liu *et al.*, "An ultra-small, low-power, all-optical flip-flop memory on a silicon chip," *Nature Photon.*, vol. 4, no. 3, pp. 182–187, Mar. 2010.
- [8] W. Zhang and J. Yao, "A fully reconfigurable waveguide Bragg grating for programmable photonic signal processing," *Nature Commun.*, vol. 9, no. 1396, Apr. 2018, Art. no. 1396.
- [9] L. Feng, R. El-Ganainy, and L. Ge, "Non-Hermitian photonics based on parity-time symmetry," *Nature Photon.*, vol. 11, no. 12, pp. 752–762, Nov. 2017.
- [10] D. J. Moss, R. Morandotti, A. L. Gaeta, and M. Lipson, "New CMOS-compatible platforms based on silicon nitride and Hydex for nonlinear optics," *Nature Photon.*, vol. 7, no. 8, pp. 597–607, Jul. 2013.
- [11] M. Y. Jing, B. Yu, J. Y. Hu, H. F. Hou, L. T. Xiao, and S. T. Jia, "Impedance self-matching ultra-narrow linewidth fiber resonator by use of a tunable π -phase-shifted FBG," *Sci. Rep.*, vol. 7, May 2017, Art. no. 1895.
- [12] A. A. Savchenkov, V. S. Ilchenko, A. B. Matsko, and L. Maleki, "Kilohertz optical resonances in dielectric crystal cavities," *Phys. Rev. A*, vol. 70, Nov. 2004, Art. no. 051804.
- [13] G. Zhao *et al.*, "Raman lasing and Fano lineshapes in a packaged fiber-coupled whispering-gallery-mode microresonator," *Sci. Bull.*, vol. 62, no. 12, pp. 875–878, Jun. 2017.
- [14] F. Auracher and R. Keil, "Method for measuring the rf modulation characteristics of Mach-Zehnder-type modulators," *Appl. Phys. Lett.*, vol. 36, no. 8, pp. 626–629, Apr. 1980.
- [15] T. Kawanishi *et al.*, "Direct measurement of chirp parameters of high-speed Mach-Zehnder-type optical modulators," *Opt. Commun.*, vol. 195, no. 6, pp. 399–404, Aug. 2001.
- [16] S. Oikawa, T. Kawanishi, and M. Izutsu, "Measurement of chirp parameters and half-wave voltages of Mach-Zehnder-type optical modulators by using a small signal operation," *IEEE Photon. Technol. Lett.*, vol. 15, no. 5, pp. 682–684, May 2003.
- [17] Y. Q. Shi, L. S. Yan, and A. E. Willner, "High-speed electrooptic modulator characterization using optical spectrum analysis," *J. Lightw. Technol.*, vol. 21, no. 10, pp. 2358–2367, Oct. 2003.
- [18] N. Courjal, J. M. Dudley, and H. Porte, "Extinction-ratio-independent method for chirp measurements of Mach-Zehnder modulators," *Opt. Express*, vol. 12, no. 3, pp. 442–448, Feb. 2004.
- [19] L. S. Yan, A. E. Willner, and Y. Q. Shi, "Graphical solution for RF half-wave voltage and chirp parameter of electrooptic modulators using optical spectrum analysis," *IEEE Photon. Technol. Lett.*, vol. 17, no. 7, pp. 1486–1488, Jul. 2005.
- [20] T. Zhang, N. H. Zhu, B. H. Zhang, and X. Zhang, "Measurement of chirp parameter and modulation index of a semiconductor laser based on optical spectrum analysis," *IEEE Photon. Technol. Lett.*, vol. 19, no. 4, pp. 227–229, Feb. 2007.
- [21] N. H. Zhu *et al.*, "Estimation of frequency response of direct modulated lasers from optical spectra," *J. Phys. D, Appl. Phys.*, vol. 39, no. 21, pp. 4578–4581, Oct. 2006.
- [22] Y. Liao, H. J. Zhou, and Z. Meng, "Modulation efficiency of a LiNbO₃ waveguide electro-optic intensity modulator operating at high microwave frequency," *Opt. Lett.*, vol. 34, no. 12, pp. 1822–1824, Jun. 2009.
- [23] Q. Y. Ye, C. Yang, and Y. H. Chong, "Improved frequency response measurement method of half-wave voltage for phase modulator," *Optik*, vol. 125, no. 2, pp. 745–747, Jan. 2014.
- [24] R. F. Bauer, and P. Penfield, "De-embedding and unterminating," *IEEE Trans. Microw. Theory Techn.*, vol. 22, no. 3, pp. 282–288, Mar. 1974.
- [25] P. D. Hale, and D. F. Williams, "Calibrated measurement of optoelectronic frequency response," *IEEE Trans. Microw. Theory Techn.*, vol. 51, no. 4, pp. 1422–1429, Apr. 2003.
- [26] N. H. Zhu *et al.*, "Microwave generation in an electro-absorption modulator integrated with a DFB laser subject to optical injection," *Opt. Express*, vol. 17, no. 24, pp. 22114–22123, Nov. 2009.
- [27] X. M. Wu *et al.*, "Novel method for frequency response measurement of optoelectronic devices," *IEEE Photon. Technol. Lett.*, vol. 24, no. 7, pp. 575–577, Apr. 2012.
- [28] X. M. Wu, J. W. Man, L. Xie, J. G. Liu, Y. Liu, and N. H. Zhu, "A new method for measuring the frequency response of broadband optoelectronic devices," *IEEE Photon. J.*, vol. 4, no. 5, pp. 1679–1685, Oct. 2012.
- [29] M. Levesque, M. Tetu, P. Tremblay, and M. Chamberland, "A novel technique to measure the dynamic response of an optical phase modulator," *IEEE Trans. Instrum. Meas.*, vol. 44, no. 5, pp. 952–957, Oct. 1995.
- [30] E. H. W. Chan, and R. A. Minasian, "A new optical phase modulator dynamic response measurement technique," *J. Lightw. Technol.*, vol. 26, no. 16, pp. 2882–2888, Aug. 2008.
- [31] S. J. Zhang, X. X. Zhang, S. Liu, and Y. Liu, "Measurement of modulation index and half-wave voltage of an electro-optical phase modulator with a dispersion-based phase filter," *Opt. Commun.*, vol. 285, no. 24, pp. 5089–5093, Nov. 2012.
- [32] Y. Q. Heng, M. Xue, W. Chen, S. L. Han, J. Q. Liu, and S. L. Pan, "Large-dynamic frequency response measurement for broadband electro-optic phase modulators," *IEEE Photon. Technol. Lett.*, vol. 31, no. 4, pp. 291–294, Feb. 2019.
- [33] M. Xue, Y. Q. Heng, and S. L. Pan, "Ultrahigh-resolution electro-optic vector analysis for characterization of high-speed electro-optic phase modulators," *J. Lightw. Technol.*, vol. 36, no. 9, pp. 1644–1649, May 2018.
- [34] T. S. Tan, R. L. Jungerman, and S. S. Elliott, "Optical receiver and modulator frequency response measurement with a Nd: YAG ring laser heterodyne technique," *IEEE Trans. Microw. Theory Techn.*, vol. 37, no. 8, pp. 1217–1222, Aug. 1989.
- [35] A. K. M. Lam, M. Fairburn, and N. A. F. Jaeger, "Wide-band electrooptic intensity modulator frequency response measurement using an optical heterodyne down-conversion technique," *IEEE Trans. Microw. Theory Techn.*, vol. 54, no. 1, pp. 240–246, Jan. 2006.
- [36] A. Chtcherbakov, R. J. Kisch, J. D. Bull, and N. A. F. Jaeger, "Optical heterodyne method for amplitude and phase response measurements for ultrawideband electrooptic modulators," *IEEE Photon. Technol. Lett.*, vol. 19, no. 1, pp. 18–20, Jan. 2007.
- [37] E. Rogers III, J. L. Carini, J. A. Pechkis, and P. L. Gould, "Characterization and compensation of the residual chirp in a Mach-Zehnder-type electro-optical intensity modulator," *Opt. Express*, vol. 18, no. 2, pp. 1166–1176, Jan. 2010.
- [38] S. J. Zhang, H. Wang, X. H. Zou, Y. L. Zhang, R. G. Lu, and Y. Liu, "Extinction-ratio-independent electrical method for measuring chirp parameters of Mach-Zehnder modulators using frequency-shifted heterodyne," *Opt. Lett.*, vol. 40, no. 12, pp. 2854–2857, Jun. 2015.
- [39] S. J. Zhang *et al.*, "Self-calibrated microwave characterization of high-speed optoelectronic devices by heterodyne spectrum mapping," *J. Lightw. Technol.*, vol. 35, no. 10, pp. 1952–1961, May 2017.
- [40] S. J. Zhang *et al.*, "Electrical probing test for characterizing wideband optical transceiving devices with self-reference and on-chip capability," *J. Lightw. Technol.*, vol. 36, no. 19, pp. 4326–4336, Oct. 2018.
- [41] S. Kawanishi and M. Saruwatari, "A very wide-band frequency response measurement system using optical heterodyne detection," *IEEE Trans. Instrum. Meas.*, vol. 38, no. 2, pp. 569–573, Apr. 1989.
- [42] J. Wang, and U. Kruger, "Measurement of frequency response of photoreceivers using self-homodyne method," *Electron. Lett.*, vol. 25, no. 11, pp. 722–723, May 1989.
- [43] M. Baney, W. V. Sorin, and S. A. Newton, "High-frequency photodiode characterization using a filtered intensity noise technique," *IEEE Photon. Technol. Lett.*, vol. 6, no. 10, pp. 1258–1260, Oct. 1994.
- [44] N. H. Zhu, J. M. Wen, H. S. San, H. P. Huang, L. J. Zhao, and W. Wang, "Improved optical heterodyne methods for measuring frequency response of photodetectors," *IEEE J. Quantum Electron.*, vol. 42, no. 3, pp. 241–248, Mar. 2006.
- [45] M. Yoshioka, S. Sato, and T. Kikuchi, "A method for measuring the frequency response of photodetector modules using twice-modulated light," *J. Lightw. Technol.*, vol. 23, no. 6, pp. 2112–2117, Jun. 2005.
- [46] K. Inagaki, T. Kawanishi, and M. Izutsu, "Optoelectronic frequency response measurement of photodiodes by using high-extinction ratio optical modulator," *IEICE Electron. Exp.*, vol. 9, no. 4, pp. 220–226, Dec. 2012.

- [47] B. Elamran, R. D. Pollard, and S. Iezekiel, "Simulation and implementation of lightwave component characterization using a bilateral electro-optic network," *IEEE Trans. Microw. Theory Tech.*, vol. 45, no. 8, pp. 1493–1496, Aug. 1997.
- [48] B. H. Zhang *et al.*, "Development of swept frequency method for measuring frequency response of photodetectors based on harmonic analysis," *IEEE Photon. Technol. Lett.*, vol. 21, no. 7, pp. 459–461, Apr. 2009.
- [49] S. J. Zhang *et al.*, "Optical frequency-detuned heterodyne for self-referenced measurement of photodetectors," *IEEE Photon. Technol. Lett.*, vol. 27, no. 9, pp. 1014–1017, May. 2015.
- [50] H. Wang *et al.*, "Two-tone intensity-modulated optical stimulus for self-referencing microwave characterization of high-speed photodetectors," *Opt. Commun.*, vol. 373, no. 15, pp. 110–113, Aug. 2016.
- [51] M. Xue, S. F. Liu, Q. Ling, Y. Q. Heng, J. B. Fu, and S. L. Pan, "Ultra-high-resolution optoelectronic vector analysis for characterization of high-speed integrated coherent receivers," *IEEE Trans. Instrum. Meas.*, vol. 69, no. 6, pp. 3812–3817, Jun. 2020.
- [52] M. K. Wang *et al.*, "Self-referenced frequency response measurement of high-speed photodetectors through segmental up-conversion based on low-speed photonic sampling," *Opt. Express*, vol. 27, no. 26, pp. 238250–38258, Dec. 2019.
- [53] T. Niemi, M. Uusimaa, and H. Ludvigsen, "Limitations of phase-shift method in measuring dense group delay ripple of fiber Bragg gratings," *IEEE Photon. Technol. Lett.*, vol. 13, no. 12, pp. 1334–1336, Dec. 2001.
- [54] G. D. Van Wiggeren, A. R. Motamedi, and D. M. Barley, "Single-scan interferometric component analyzer," *IEEE Photon. Technol. Lett.*, vol. 15, no. 2, pp. 263–265, Feb. 2013.
- [55] D. K. Gifford, B. J. Soller, M. S. Wolfe, and M. E. Froggatt, "Optical vector network analyzer for single-scan measurements of loss, group delay, and polarization mode dispersion," *Appl. Opt.*, vol. 44, no. 34, pp. 7282–7286, Dec. 2005.
- [56] X. W. Yi, W. Shieh, and Y. Ma, "Phase noise effects on high spectral efficiency coherent optical OFDM transmission," *J. Lightw. Technol.*, vol. 26, no. 10, pp. 1309–1316, May 2008.
- [57] W. Shieh, R. S. Tucker, W. Chen, X. W. Yi, and G. Pendock, "Optical performance monitoring in coherent optical OFDM systems," *Opt. Express*, vol. 15, no. 2, pp. 350–356, Jan. 2007.
- [58] F. N. Hauske, M. Kuschnerov, B. Spinnler, and B. Lankl, "Optical performance monitoring in digital coherent receivers," *J. Lightw. Technol.*, vol. 27, no. 16, pp. 3623–3631, Aug. 2009.
- [59] M. S. Faruk, Y. Mori, C. Zhang, K. Igarashi, and K. Kikuchi, "Multi-impairment monitoring from adaptive finite-impulse-response filters in a digital coherent receiver," *Opt. Express*, vol. 18, no. 26, pp. 26929–26936, Dec. 2010.
- [60] X. W. Yi, Z. H. Li, Y. Bao, and Q. K. Qiu, "Characterization of passive optical components by DSP-based optical channel estimation," *IEEE Photon. Technol. Lett.*, vol. 24, no. 6, pp. 443–445, Mar. 2012.
- [61] C. Jin *et al.*, "High-resolution optical spectrum characterization using optical channel estimation and spectrum stitching technique," *Opt. Lett.*, vol. 38, no. 13, pp. 2314–2316, Jul. 2013.
- [62] Z. H. Li and X. W. Yi, "Spectral characterization of passive optical devices," *Proc. SPIE Newsroom Sens. Meas.*, pp. 1–3, Feb. 2014.
- [63] R. Hernández, A. Loayssa, and D. Benito, "Optical vector network analysis based on single-sideband modulation," *Opt. Eng.*, vol. 43, no. 10, pp. 2418–2421, Mar. 2004.
- [64] D. J. Krause, J. C. Cartledge, L. Jakober, and K. Roberts, "Measurement of passive optical components using a carrier and single sideband," in *Proc. Opt. Fiber Commun. Conf.*, Anaheim, CA, USA, 2006, Paper OFN5.
- [65] M. Sagues, G. Beloki, and A. Loayssa, "Broadband swept optical single-sideband modulation generation for spectral characterization of optical components," in *Proc. 33rd Eur. Conf. Exhib. Opt. Commun.*, Berlin, Germany, Sep. 2007.
- [66] M. Sagues and A. Loayssa, "Spectral characterisation of polarisation dependent loss of optical components using optical single sideband modulation," *Electron. Lett.*, vol. 47, no. 1, pp. 47–49, Jan. 2011.
- [67] A. Loayssa, R. Hernández, D. Benito, and S. Galech, "Characterization of stimulated Brillouin scattering spectra by use of optical single-sideband modulation," *Opt. Lett.*, vol. 29, no. 6, pp. 638–640, Mar. 2004.
- [68] Z. Tang, S. Pan, and J. Yao, "A high resolution optical vector network analyzer based on a wideband and wavelength-tunable optical single-sideband modulator," *Opt. Express*, vol. 20, no. 6, pp. 6555–6560, Mar. 2012.
- [69] M. Sagues and A. Loayssa, "Swept optical single sideband modulation for spectral measurement applications using stimulated Brillouin scattering," *Opt. Express*, vol. 18, no. 16, pp. 17555–17568, Jul. 2010.
- [70] M. Xue, S. Pan, and Y. Zhao, "Accuracy improvement of optical vector network analyzer based on single-sideband modulation," *Opt. Lett.*, vol. 39, no. 12, pp. 3595–3598, Jun. 2014.
- [71] M. Xue, S. L. Pan, and Y. Zhao, "Accurate optical vector network analyzer based on optical single-sideband modulation and balanced photodetection," *Opt. Lett.*, vol. 40, no. 4, pp. 569–572, Feb. 2015.
- [72] W. T. Wang, W. Li, J. G. Liu, W. H. Sun, W. Y. Wang, and N. H. Zhu, "Optical vector network analyzer with improved accuracy based on Brillouin-assisted optical carrier processing," *IEEE Photon. J.*, vol. 6, no. 6, Dec. 2014, Art. no. 5501310.
- [73] W. Li, W. H. Sun, W. T. Wang, L. X. Wang, J. G. Liu, and N. H. Zhu, "Reduction of measurement error of optical vector network analyzer based on DPMZM," *IEEE Photon. Technol. Lett.*, vol. 26, no. 9, pp. 866–869, May 2014.
- [74] W. Li, J. G. Liu, and N. H. Zhu, "Optical vector network analyzer with improved accuracy based on polarization modulation and polarization pulling," *Opt. Lett.*, vol. 40, no. 8, pp. 1679–1682, Apr. 2015.
- [75] M. Xue, S. Pan, and Y. Zhao, "Optical spectral response measurement based on optical single-sideband modulation with doubled measurement range," *Electron. Lett.*, vol. 52, no. 10, pp. 852–853, May. 2016.
- [76] M. Xue, S. Pan, C. He, R. Guo, and Y. Zhao, "Wideband optical vector network analyzer based on optical single-sideband modulation and optical frequency comb," *Opt. Lett.*, vol. 38, no. 22, pp. 4900–4902, Nov. 2013.
- [77] W. Li, W. T. Wang, L. X. Wang, and N. H. Zhu, "Optical vector network analyzer based on single-sideband modulation and segmental measurement," *IEEE Photon. J.*, vol. 6, no. 2, Apr. 2014, Art. no. 790110.
- [78] M. Wang and J. Yao, "Optical vector network analyzer based on unbalanced double-sideband modulation," *IEEE Photon. Technol. Lett.*, vol. 25, no. 8, pp. 753–756, Apr. 2013.
- [79] T. Qing, S. Li, M. Xue, and S. Pan, "Optical vector analysis based on double-sideband modulation and stimulated Brillouin scattering," *Opt. Lett.*, vol. 41, no. 15, pp. 3671–3674, Aug. 2016.
- [80] T. Qing, M. Xue, M. Huang, and S. L. Pan, "Measurement of optical magnitude response based on double-sideband modulation," *Opt. Lett.*, vol. 39, no. 21, pp. 6174–6176, Nov. 2014.
- [81] T. Qing, S. Li, M. Xue, W. Li, N. H. Zhu, and S. Pan, "Optical vector analysis based on asymmetrical optical double-sideband modulation using a dual-drive dual-parallel Mach-Zehnder modulator," *Opt. Express*, vol. 25, no. 5, pp. 4665–4671, Mar. 2017.
- [82] X. Zou *et al.*, "Hyperfine intrinsic magnitude and phase response measurement of optical filters based on electro-optical harmonics heterodyne and Wiener-Lee transformation," *J. Lightw. Technol.*, vol. 37, no. 11, pp. 2654–2660, Jun. 2019.
- [83] J. Wen *et al.*, "Optical vector network analyzer based on double-sideband modulation," *Opt. Lett.*, vol. 42, no. 21, pp. 4426–4429, Nov. 2017.
- [84] T. Su *et al.*, "Wideband optical vector network analyzer based on polarization modulation," *Opt. Commun.*, vol. 437, pp. 67–70, Apr. 2019.
- [85] M. Xue, S. Liu, and S. Pan, "High-resolution optical vector analysis based on symmetric double-sideband modulation," *IEEE Photon. Technol. Lett.*, vol. 30, no. 5, pp. 491–494, Mar. 2018.
- [86] S. Liu, M. Xue, J. Fu, L. Wu, and S. Pan, "Ultra-high-resolution and wideband optical vector analysis for arbitrary responses," *Opt. Lett.*, vol. 43, no. 4, pp. 727–730, Feb. 2018.
- [87] J. Wen *et al.*, "Accuracy-enhanced wideband optical vector network analyzer based on double-sideband modulation," *J. Lightw. Technol.*, vol. 37, no. 13, pp. 2920–2926, Jul. 2019.
- [88] R. M. Craig, S. L. Gilbert, and P. D. Hale, "High-resolution, nonmechanical approach to polarization-dependent transmission measurements," *J. Lightw. Technol.*, vol. 16, no. 7, pp. 1285–1294, Jul. 1998.
- [89] M. Sagues, M. Pérez and A. Loayssa, "Measurement of polarization dependent loss, polarization mode dispersion and group delay of optical components using swept optical single sideband modulated signals," *Opt. Express*, vol. 16, no. 20, pp. 16181–16188, Sep. 2008.
- [90] B. L. Heffner, "Deterministic, analytically complete measurement of polarization-dependent transmission through optical devices," *IEEE Photon. Technol. Lett.*, vol. 4, no. 5, pp. 451–454, May 1992.
- [91] T. Qing *et al.*, "Optical vector analysis with attometer resolution, 90-dB dynamic range and THz bandwidth," *Nat. Commun.*, vol. 10, Nov. 2019, Art. no. 5135.
- [92] B. Elamran, R. D. Pollard, and S. Iezekiel, "Implementation and calibration of a two-port electrooptic network analyzer," *IEEE Microw. Guided Wave Lett.*, vol. 9, no. 9, pp. 369–371, Sep. 1999.

- [93] B. Elamaram, R. D. Pollard and S. Iezekiel, "A bilateral lightwave network analyzer-architecture and calibration," *IEEE Trans. Microw. Theory Techn.*, vol. 48, no. 12, pp. 2630–2636, Dec. 2000.
- [94] D. Frolov, A. Levchenko, and K. Korotkov, "Extracting S-parameters of bilateral electro-optic network for lightwave component analyzer calibration," *J. Phys. Conf. Ser.*, vol. 643, no. 1, Apr. 2015, Art. no. 012062.
- [95] S. Iezekiel, B. Elamaram, and R. D. Pollard, "Recent developments in lightwave network analysis," *Eng. Sci. Educ. J.*, vol. 9, no. 6, pp. 247–257, Dec. 2000.
- [96] K. Silvonen, N. H. Zhu, and Y. Liu, "A 16-term error model based on linear equations of voltage and current variables," *IEEE Trans. Microw. Theory Techn.*, vol. 54, no. 4, pp. 1464–1469, Apr. 2006.
- [97] N. H. Zhu, "Phase uncertainty in calibrating microwave test fixtures," *IEEE Trans. Microw. Theory Techn.*, vol. 47, no. 10, pp. 1917–1922, Oct. 1999.
- [98] A. L. Waksberg, M. H. Hubert, and W. R. L. Clements, "Laser modulation depth determination by a simple power measuring technique," *IEEE J. Quantum Electron.*, vol. 12, no. 11, pp. 734–736, Nov. 1976.
- [99] S. Uehara, "Calibration of optical modulator frequency response with application to signal level control," *Appl. Opt.*, vol. 17, no. 1, pp. 68–71, Jan. 1978.
- [100] H. P. Huang *et al.*, "Small-signal power measuring technique for measuring the frequency response of electroabsorption modulators," *IEEE Photon. Technol. Lett.*, vol. 18, no. 23, pp. 2451–2453, Dec. 2006.
- [101] R. T. Hawkins, M. D. Jones, S. H. Pepper, and J. H. Goll, "Comparison of fast photodetector response measurements by optical heterodyne and pulse response techniques," *J. Light. Technol.*, vol. 9, no. 10, pp. 1289–1294, Oct. 1991.
- [102] S. L. Pan and J. P. Yao, "Photonics-based broadband microwave measurement," *J. Lightw. Technol.*, vol. 35, no. 16, pp. 3498–3513, Aug. 2017.
- [103] D. F. William *et al.*, "Covariance-based uncertainty analysis of the NIST electrooptic sampling system," *IEEE Trans. Microw. Theory Techn.*, vol. 54, no. 1, pp. 481–490, Jan. 2006.
- [104] T. Dennis and P. D. Hale, "High-accuracy photoreceiver frequency response measurements at 155 μm by use of a heterodyne phase-locked loop," *Opt. Express*, vol. 19, no. 21, pp. 20103–20114, Oct. 2011.

Shangjian Zhang (Member, IEEE) received the Ph.D. degree from the Institute of Semiconductors, Chinese Academy of Sciences (CAS), in 2006. He was a Visiting Researcher at COBRA, Eindhoven University of Technology, the Netherlands, and University of California, Santa Barbara, USA. He is a Full Professor with the University of Electronic Science and Technology of China. Dr. Zhang has authored or coauthored over 140 papers and holds 19 patents. His research interests include high-speed optoelectronic integrated devices and microwave photonic instrumentation.

Wei Li (Member, IEEE) received the Ph.D. degree in microelectronics and solid-state electronics from the Institute of Semiconductors, Chinese Academy of Sciences (CAS), Beijing, China, in 2010. He is currently a Full Professor with the Institute of Semiconductors, CAS. His research interests include high-frequency characteristics of optoelectronic devices, radars, and microwave photonics. Prof. Li was the recipient of the Humboldt Research Fellowship from the Alexander von Humboldt Foundation, Germany (2011–2012).

Wei Chen received the B.S. degree in physics from Beijing Normal University, Beijing, China, in 2004, and the Ph.D. degree in opto-electronics from the Institute of Semiconductors, Chinese Academy of Sciences (CAS), Beijing, China. His research interests are optical fiber resonators, Brillouin erbium-doped fiber lasers, and design of high-speed electroabsorption-modulated laser (EML) transmitter optical subassembly (TOSA).

Yali Zhang received the Ph.D. degree from the Institute of Semiconductors, Chinese Academy of Sciences. She is currently an Associate Professor with the School of Optoelectronic Science and Engineering from the University of Electronic Science and Technology of China. Her research interests include optical communications and integrated optics and microwave photonics.

Ninghua Zhu (Member, IEEE) received the B.S., M.S., and Ph.D. degrees in electronic engineering from the University of Electronic Science and Technology of China, Chengdu, China, in 1982, 1986, and 1990, respectively. From 1990 to 1994, he was a Postdoctoral Fellow with Zhongshan University, Guangzhou, China, where he became an Associate Professor in 1992 and a Full Professor in 1994. From 1994 to 1995, he was a Research Fellow with the Department of Electronic Engineering, City University of Hong Kong. From 1996 to 1998, he was with the Siemens Corporate Technology, Munich, Germany, as a Guest Scientist (Humboldt Fellow), where he was involved in the microwave design and testing of external waveguide modulators and laser modules. He is currently a Professor with the Institute of Semiconductors, Chinese Academy of Sciences (CAS), Beijing, China. In 1998, he was with the Hundred-Talent Program, CAS, and was selected by the National Natural Science Foundation as a Distinguished Young Scientist. He has authored or coauthored more than 200 journal papers, three books, and three book chapters. He additionally holds 90 patents. His research interests include modeling and characterization of integrated optical waveguides and coplanar transmission lines, and optimal design of optoelectronics devices and photonic integrated circuits. Prof. Zhu is a leader in the field of optoelectronics in China. In cooperation with Huawei, ZTE, and Guangxun (the fourth largest optical device in the world), he has developed a variety of lasers, and achieved mass production and applications of high-performance chips. The annual output of Guangxun has exceeded one billion yuan. The developed laser, as the core light source of satellite laser communication, is in orbit among Beidou navigation satellites. As the first complete person, he was the recipient of the 2013 and 2018 National Award for Technological Invention Second Prize. He also won three Provincial and Ministerial First Prizes, Guanghua Engineering Award and the Chinese Academy of Sciences Outstanding Achievement Award (individual). He used to be the Ministry of Science and Technology as a member of "863" project, and now he is the leader of the National key research and development program Optoelectronics and Microelectronic Devices and Integration.